ELEVATED TEMPERATURE, RESIDUAL COMPRESSIVE STRENGTH OF IMPACT-DAMAGED SANDWICH STRUCTURE MANUFACTURED OUT-OF-AUTOCLAVE†

Brian W. Grimsley[1], James K. Sutter[2], Eric R. Burke[1], Genevieve D. Dixon[1], Thomas G. Gyekenyesi[2], and Stanley S. Smeltzer[1]

[1] NASA Langley Research Center, Hampton, VA 23681
[2] NASA Glenn Research Center, Cleveland, OH 44135

ABSTRACT

Several 1/16th-scale curved sandwich composite panel sections of a 10 m diameter barrel were fabricated to demonstrate the manufacturability of large-scale curved sections using minimum gauge, $[+60/-60/0]_S$, toughened epoxy composite facesheets co-cured with low density (50 kg/m^3) aluminum honeycomb core. One of these panels was fabricated out of autoclave (OoA) by the vacuum bag oven (VBO) process using Cycom® T40-800b/5320-1 prepreg system while another panel with the same lay-up and dimensions was fabricated using the autoclave-cure, toughened epoxy prepreg system Cycom® IM7/977-3. The resulting 2.44 m x 2 m curved panels were investigated by non-destructive evaluation (NDE) at NASA Langley Research Center (NASA LaRC) to determine initial fabrication quality and then cut into smaller coupons for elevated temperature wet (ETW) mechanical property characterization. Mechanical property characterization of the sandwich coupons was conducted including edge-wise compression (EWC), and compression-after-impact (CAI) at conditions ranging from 25°C/dry to 150°C/wet. The details and results of this characterization effort are presented in this paper.

1. INTRODUCTION

NASA is currently developing a Heavy Lift - Space Launch System (HL-SLS) with an initial lift capability of 70-100 mT and evolvable up to 130 mT. The design for the payload shroud of this system has included studies of both metallic semi-monocoque and honeycomb sandwich carbon fiber reinforced polymer (CFRP) composite structure. While the aluminum-lithium (Al-Li) alloys used in metallic structure are a well understood and certified material for use in launch systems[1,2], the high strength-to-weight and stiffness-to-weight characteristics of CFRP sandwich make it an attractive alternative to Al-Li alloys especially in the lightly-loaded, complex curvature geometry of the proposed HL-SLS shroud architecture. The use of stiff, lightweight CFRP sandwich structure nominally translates into an increased payload capacity resulting in a higher performance launch system. In addition to the improved performance that could be realized by using an aerospace certified toughened epoxy CFRP processed in autoclave, the aerospace materials industry has recently developed an aerospace CFRP prepreg system that can be processed out-of-autoclave (OoA), thereby significantly lowering the costs associated with fabrication of these lightweight structures. The state-of-art in high-throughput fabrication of

aerospace quality CFRP structure using toughened epoxy prepreg tape like the Cycom® IM7/977-3 system requires that the robotically placed part be vacuum-bagged and cured under elevated temperature (≈ 120°C) and pressure (≈ 690 kPa) in an autoclave. Large autoclaves are very expensive to operate and there are currently no commercially available autoclaves in the U.S large enough to process a full 10 m barrel. For a shroud structure, which is intended to be assembled in sections, or petals, there are a limited number of industry autoclaves with sufficient diameter and length to fabricate a $1/6^{th}$ scale section of the 130 mT payload shroud. The newly developed Cycom® 5320-1 system is a class of toughened epoxy matrix, which, among others, when processed into carbon fiber reinforced prepreg tape, can be robotically placed on rigid tooling and then oven cured under a vacuum bag using only atmospheric pressure (101 kPa) in the OoA fabrication of both monocoque and sandwich CFRP structure. Initial studies [3-5] have demonstrated that the resulting thermal and mechanical properties of these new OOA CFRP are comparable, if not equivalent, to autoclave processed toughened epoxy CFRP. These positive initial results indicate that the OoA CFRP systems have the potential to significantly lower the cost to manufacture large-scale CFRP structure for commercial, military, and space flight vehicles. While CFRP sandwich offer a light-weight alternative to metallic structure, the lower damage resistance and tolerance inherent to CFRP structure results in a design allowable knockdown [6]. The ability to predict strength retention of CFRP after impact events such as barely visible impact damage (BVID) is thus of significant importance and this subject has received some attention in the literature [7-12]. However, the damage tolerance of CFRP sandwich structure for the purpose of design is currently determined experimentally [13].

1.1 Residual Compressive Strength and Failure Mechanisms of Impact-Damaged Sandwich Panels

CFRP sandwich are susceptible to damage from out-of-plane loading, including low-velocity impact [14]. These structures must be designed to sustain ultimate load with BVID, in case the damage is not detected and repaired prior to service. BVID for commercial aircraft is defined by the Boeing Company as small damages which may not be found during heavy-maintenance, general visual inspections using typical lighting conditions from a distance of 1.5 m and having a dent depth of 0.25 mm to 0.51 mm at the Outer Mold Line [15] and it is the damage state that establishes the design strength values to be used in analyses demonstrating compliance with the regulatory ultimate load requirements of FAR 25.305 [16]. According to the Federal Aviation Administration (FAA), foreign object impact is a concern for most composite structures, requiring attention in the damage threat assessment. This is needed to identify impact damage severity and detectability for design and maintenance. The assessment should include any available damage data collected from service plus an impact survey consisting of impact tests performed with representative structure. BVID is defined in this document as the likely impact damage at the threshold of reliable detection. [17] NASA has defined the minimum impact damage from low-released-mass-parts, or tool-drop, inflicted on a composite component during full-scale damage tolerance testing shall be at least that caused by a 1.0 inch diameter impactor at 136 N-m of kinetic energy or a dent 2.54 mm deep, whichever is smaller [18]. BVID can result in a compressive strength reduction of up to 50% relative to an undamaged structure [19]. In this previous study conducted by Jackson comparing undamaged, impact-damaged, and open-hole flat CFRP sandwich specimens consisting of woven fabric/toughened epoxy face-sheets, the mechanisms, or process which leads to final failure, of these structure loaded in axial compression is explained. The study[19] also included face-sheet thickness as a factor in

determining these failure mechanisms with testing of 15.24 cm x 15.24 cm specimens having two plies of prepreg fabric in the facesheets and specimens with four prepreg fabric plies. In edge-wise compression (EWC) testing the 2-ply (0.4 mm thick facesheets) undamaged specimens were found to fail by delamination of plies within the facesheets. The outer ply was observed to buckle, or wrinkle, outward, while the inner ply displayed a combination of buckling inward and outward across the width. The 2.54 cm thick core material was varied in this previous study as well, including 50 kg/m^3 Nomex and 98 kg/m^3 Al-honeycomb with 3.18 mm hexagonal cells. The results indicated that the core material in the undamaged specimens did not affect the compressive failure response, indicating that the axial loading capability in the undamaged coupons is dominated by the strength of the CFRP facesheets. However, in the damaged coupons, analysis of the strain distributions around the damage indicated that the calculated load ratio between a damaged area and an undamaged area of the facesheets bonded to the stiffer Al honeycomb core were much more stable up to failure than the coupons containing the Nomex® core. In this previous study, for the 2-ply facesheet sandwich specimens with Nomex core, the BVID damage was defined to be damage resulting using a 1.27 cm diameter indenter. This resulted in reported average dent-depths of 0.81 mm and 1.04 mm. At this level of BVID, a small region of broken fibers was observed in the surface ply at the center of the impact area. In the compression after impact (CAI) testing, observations reported for the damaged sandwich coupons with 2-ply facesheets was different than the failure mechanisms observed in the 4-ply facesheet sandwich structure specimens. During compression loading, monitoring of the out-of-plane displacements by interferometry indicated that the failure mechanism in the 2-ply facesheet coupons began with inward buckling in a circular pattern of the facesheet at the impact region. With increasing load, the circular pattern of the inward buckling expanded, taking on an elliptical shape of inward buckling spanning the width of the test specimen [19]. Failure occurred across the specimen width along the horizontal axis of the observed elliptical depression. The surface surrounding the fracture line of the 2-ply facesheet was buckled inward. In the 4-ply facesheet (0.8mm thick) BVID specimens, the failure mechanism was very similar to open-hole fracture behavior, where very little out-of-plane deformation occurred until visible damage initiated at the edges of the BVID area at approximately 90% of compressive failure load. With increased loading, the visible damage then grew in-plane, horizontally outwards towards the edges of the specimen. In these 4-ply facesheet specimens, ultimate compressive failure resulted in the fibers buckled outward rather than inward as observed in the 2-ply facesheet sandwich specimens. The failure mechanisms and ultimate failure modes associated with CAI of BVID sandwich CFRP described in this previous work provide a framework for the current study presented in the following pages. However, while the failure modes are discussed below in the results, the out-of-plane displacements of the undamaged and damaged CFRP sandwich specimens are beyond the scope of the current study to determine and compare the elevated temperature wet (ETW) retention of compressive strength of autoclave versus OoA fabricated curved sandwich structure.

1.2 Elevated Temperature Wet CFRP performance

With a predicted max speed of Mach 7, the barrel portion of the HL-SLS shroud structure is anticipated to reach maximum temperatures from aerodynamic heating of 204°C (400°F). A cork thermal protection system (TPS) is currently proposed to maintain the structure (either the metallic or CFRP sandwich) below 150°C, adding significant weight to this large structure. At elevated temperatures, the stiffness of the organic polymer matrix in the CFRP facesheets will decrease due to increased polymer chain mobility[20]. In addition, the fabricated CFRP

sandwich structure will absorb moisture during shipment, assembly, and staging prior to launch at NASA Kennedy Space Center (KSC). The surfaces of the launch vehicle are exposed to relative humidity exceeding 90% during pre-launch on the pad at KSC. This high-humidity environment increases the absorption of moisture in the CFRP. Water molecules have a plasticizing effect on the epoxy polymer and result in swelling of the matrix surrounding the stiff carbon fibers. The swelling of the matrix results in an increase in the strains and accompanying stresses at the polymer-fiber interface; both phenomena result in a decrease in the mechanical performance of the CFRP sandwich structure [21]. The Cycom® IM7/977-3 CFRP has a reported dry glass transition temperature (dry-T_g) of 235°C [22] and a wet-T_g of 194°C [20] measured from the tan-delta peak in dynamic mechanical analysis(DMA). The Cycom® 5320-1 dry-Tg has been determined to be 195°C at the knee in the E' curve from DMA [23]. The wet-Tg of Cytec 5320-1 has been reported as 164°C [24]. The upper-use-temperature of composite materials is often defined as 28°C (50°F) below the wet-T_g [20]. This arbitrary, or " rule of thumb", value is often used in design of CFRP structure to account for variability in the reporting of T_g and ensure that the material retains a significant degree of stiffness and strength at the proposed elevated temperature wet (ETW) operating conditions. Normally, it is desirable that the material retain greater than 50% of its certified ambient mechanical properties at the intended operating temperature [25].

2. EXPERIMENTAL

2.1 Materials and Test Coupon Preparation

The 2.44 m x 2 m curved panels were fabricated at HITCO Carbon Composites, Inc®, Gardena, CA by automated tape placement (ATP) of 15.2 cm wide prepreg tape onto a rigid composite tool. The part was then vacuum bagged and cured either in autoclave or in an oven using the OoA, VBO process. The autoclave processed curved sandwich panel, designated manufactured test panel 6003 (MTP-6003), contained $[+60/-60/0]_S$ facesheets of Cycom® IM7/977-3 supplied by Cytec Engineered Materials® Greenville, TX. The OoA processed curved sandwich panel, designated MTP-6010, was fabricated using $[+60/-60/0]_S$ facesheets of Cycom®T40-800b/ 5320-1 VBO prepreg. The resulting CFRP facesheets from both panels were determined by microscopy to have an average thickness of 0.76 mm [23]. Both panels were co-cured with 2.9 cm thick, 50 kg/m^3 aluminum vented honeycomb core provided by Alcore, Inc.® Edgewood, MD and Cycom® FM-300 core bondline film. The FM-300 film has a wet Tg of 126°C reported by Cytec® from the tan-delta peak in DMA. Panel MTP-6003 was processed using a Cytec peel ply designated as 600001 dry peel ply. This peel ply did not release from the panel surfaces after autoclave cure. Upon arrival of the panels at LaRC, non-destructive evaluation (NDE) by pitch-and-catch UT-scan and flash-IR thermography indicated that the two panels contained few flaws and could proceed into test coupon preparation; any flaws identified were worked around.

The cut pattern and coupon labels for panel MTP-6003 are displayed in Figure 1. For brevity, the cut pattern for MTP-6010 is not shown, but is similar to MTP-6003, except that the 0.9 m x 1.5 m buckling panel was shifted to the left edge of the 2.4 m x 2 m fabricated panel to avoid flaws detected on the right edge during NDE. The 0.9 m x 1.5 m curved specimen was removed from each panel for compressive testing as part of a separate buckling analysis study. All of the 20.95 cm x 15.88 cm EWC and CAI coupons were rough-cut from the large panel using a diamond-grit band-saw blade. The 20.95 cm dimension was cut parallel to the 0° fibers in the panel and the 15.88 cm dimension parallel to the circumference of the curved panel. This put the 0° fibers

parallel to the direction of compressive loading during testing. After rough cutting, the specimens were machined to the nominal 20.32 cm x 15.24 cm dimension following specifications in ASTM C364 [26] using a diamond-grit end mill. In preparation for potting, a carbide end-mill was used to machine away a 1.27 cm depth of the 2.9 cm thick aluminum core from each end of the specimen. This process left less than 1.27 mm of core and core bondline film bonded to the inner surfaces of the facesheets at the potted ends.

The 20.32 cm x 15.24 cm curved EWC and CAI specimens were potted using Henkel® Hysol EA934NA epoxy potting compound following the supplier recommended bonding procedures. This resulted in a solid block of potting at each end of the specimen having dimensions of 17.8 cm x 5.4 cm x 1.6 cm. Photographs of the front-view and side-view of the potted coupon are displayed in Figure 2 and Figure 3, respectively. After the potting material cured at 25°C for 7 days, the ends of each potted specimen were machined to remove 3.175 mm from each end to ensure that the CFRP facesheets were flush with the surface of the potting material and that the potted ends were parallel to each other within +/-0.0254 mm. A photograph of the top-view of the potted specimen is shown in Figure 4.

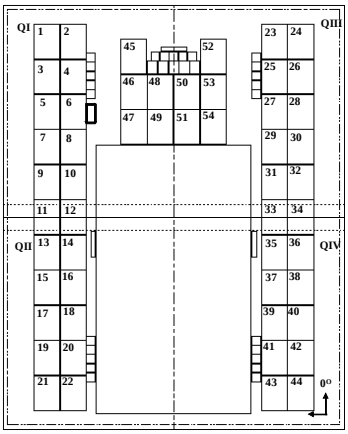

Figure 1. Schematic of panel MTP 6003 showing EWC and CAI coupon rough cutting diagram and numbering methodology.

Figure 2. Front-view photograph of potted EWC and/or CAI test coupon.

Figure 3. Side-view photograph of potted EWC and/or CAI test coupon.

Figure 4. Top-view photograph of potted EWC and/or CAI test coupon.

2.2 BVID Impact of CAI Specimens

After potting, the 20.32 cm x 15.24 cm curved CAI test coupons were centered and clamped in an existing 12.7 cm square aluminum picture-frame using polyethylene shims to account for coupon curvature. Following ASTM D7136 [27], dynamic impacting at the center of the convex facesheet of the CAI test coupons was performed in a drop tower using an instrumented impactor weighing 3.03 kg. The impactor consisted of a 1.27 cm diameter hemispherical indenter and a Dynatup load cell attached to a cylindrical mass. Different drop heights were used on several trial coupons from MTP-6003 until an impact energy of 2.03 N-m (1.5 ft-lb) resulted in BVID, according to the Boeing Company criteria found in the literature and presented earlier in the Introduction section. This impact energy resulted in damage which was barely visible from a distance of 1.5 m with an average dent depth of 0.76 mm (0.03 in) as measured using a dial gauge. Once the BVID impact energy was determined using several sample coupons from MTP-6003, for efficacy, instrumented impacts were performed on 24 CAI test coupons from panel MTP6003 and 24 CAI test coupons from MTP 6010. One coupon from each of the panels was randomly selected for NDE analysis of the impact site by micro-focused x-ray computed tomography (micro-CT) using an XTech ® micro-CT with volume-pixel setting of 0.33 mm in all directions.

2.3 Coupon gauging and Conditioning

Following the recommendation in ASTM C364 [26], all 100 EWC and CAI test coupons were instrumented using CEA-XX-187UW-350, 4.75 mm uniaxial strain gages supplied by Vishay Micro-Measurements®, Raleigh, NC. As indicated in Figure 2, two gauges were used on each side of the coupons, each located in the lower corners, 2.54 cm above the potting and 2.54 cm from the vertical edge of the coupon. These 4 gauges on each coupon were monitored during compression testing to ensure parallel loading and inhibit bending. The 27 coupons intended for ambient testing were gauged at LaRC according to procedures specified by the gauge supplier.

The remaining 73 coupons intended for ETW EWC and CAI were instrumented at Modern Machine and Tool, Inc®, Newport News, VA using identical Vishay gauges, but with the additional step of applying multiple coats of Vishay® m-coat-J, an RTV-like material to protect the gauges and solder joints during the moisture conditioning of the coupons.

Following ASTM D5229 [28], the coupons selected for ETW testing from panels MTP-6003 and MTP-6010 were placed in a laboratory conditioning chamber for approximately 50 days to reach the equilibrium moisture saturation state. Space limitations in the Tenney Environmental® VersaTenn III conditioning chamber dictated that the conditioning and testing process be staggered until all 73 coupons could be conditioned following the same procedures. Beginning with the MTP-6003 panel, 35 ETW coupons were placed in the chamber such that at least 2.54 cm spacing existed between surfaces of coupon facesheets. In addition, a 10.2 cm x 5.1cm sandwich witness coupon cut from quadrant (Q1) of MTP-6003 and MTP-6010 was held within the center of the chamber amongst the test coupons, allowing it to be accessed periodically to measure the moisture absorption of each set of coupons. The chamber was programmed to continuously provide a heated, relative humidity (RH) environment of 80°C / 85%RH. Using a Mettler Toledo® micro-balance, the witness coupon accompanying each batch of coupons was weighed daily during the first five days of conditioning and then once weekly until the plotted data indicated that the mass gain had stabilized. At each weighing period, the witness coupon mass was measured five times and the average reported. Once the coupons reached moisture equilibrium, testing began. The untested coupons from each conditioning batch remained in the chamber at 80°C/85%RH and the witness coupon continued to be weighed until all testing was completed. The testing of the 35 ETW specimens required approximately ten days. The 27 potted and gauged EWC and CAI coupons intended for ambient-dry testing were conditioned in a convective oven at 71.1°C for 120 hrs without an accompanying witness coupon.

2.4 Compression Testing

Following ASTM C364 for the EWC testing and reference [19] for the sandwich CFRP CAI testing, the 100 potted and gauged coupons were loaded to failure in a 50 kN MTS® hydraulic test stand. The coupons were centered between 10.2 cm thick steel bearing platens determined to be parallel within 0.051 mm. The top surface of the potted coupon was separated from the top platen by a 17.8 cm x 5.4 cm shim of flat 1.3 cm thick aluminum plate to adequately distribute the compressive load after any shimming deemed necessary to prevent bending. Because of the sandwich geometry of the coupons, no side supports were required to prevent global buckling. Initial compression loading of several EWC coupons indicated that the width and flatness of the end-potting was sufficient and no clamps were required. For the safety of the test operator, 1.8 m tall plexiglass screens surrounded the test frame during loading at 25°C. Since compressive strength is sensitive to even minor misalignments and to ensure parallel loading of the coupons, the following crosshead alignment procedures were used for each EWC and CAI coupon tested:

1. The potted test coupon was placed on the marked centerline of the lower compression platen and the four corner strain gages were wired to the data acquisition system.
2. The 1.3 cm thick al shim plate was centered on the top of the potted coupon.
3. The platens were closed at 0.51 mm/min until a load of 22 N (5 lbf) was reported by the load cell.
4. The 4 corner strain gages were checked via the data acquisition system.

5. If the strains indicated by the 4 gauges differed by more than 5%, 0.013 mm thick steel shim-stock was inserted between the upper platen and the Al shim plate until the strain differential was less than 5%.
6. The platens were then closed at a rate of 0.51 mm/min until a load of 30% of failure load, approximately 9 kN (2,000 lbf), and the difference in strain reported by the corner gages was verified to be < 5%.
7. The load was then released at a rate of 0.51 mm/min until the load cell returned to 22 N.
8. For EWC or CAI at 25°C-dry and/or 25°C-wet, compression testing begins.

For the ETW testing, the saturated coupons were removed one-at-a-time from the moisture conditioning chamber and allowed to cool from 80°C to the testing laboratory temperature of 25°C before commencing the crosshead alignment procedures; this cooling step duration was nominally 30 min. After shimming in the test frame, process thermocouples were attached using Kapton tape to the center of both CFRP facesheets, with the bead covered by a 1.27 cm x 2.54 cm x 0.64cm piece of silicon bagging tape adhered to the surface of the facesheets. The coupon and platens were enclosed in a convective oven designed for elevated temperature mechanical characterization by MTS Environmental ® (Model # 651).

After the thermocouple bonding step, the heating chamber was programmed to heat at a rate of 5°C/min to the desired test temperature and dwell. When the process thermocouples indicated that the surface of both the concave and convex facesheets had reached the test temperature, the specimen was held at this temperature for 2 mins and the compression test was started.

The coupon was then loaded to failure in displacement-control at a rate of 0.51 mm/min. Load, displacement, strain, and temperature (ETW testing only) was continuously recorded by the digital data acquisition system. Between three and five replicate tests were conducted for each test condition as dictated by coupon availability. At each condition, coupons were selected from multiple panel quadrants, as shown in Figure 1 above.

3. RESULTS AND DISCUSSION

Following the steps detailed in the Experimental Section, 25 of the IM7/977-3 autoclave-fabricated, undamaged sandwich coupons from panel MTP-6003 and 19 of the T40-800b/5320-1 OOA fabricated, undamaged sandwich coupons from panel MTP-6010 were tested in edgewise compression at ETW conditions ranging from 25°C-wet to 150°C-wet to provide a basis for judging the load carrying capacity of the sandwich construction in terms of developed facing stress. In addition, 24 coupons from MTP-6003 and 14 coupons from MTP-6010 were impacted to a level of BVID and tested in edgewise compression in the same range of ETW conditions to determine the CAI strength and compare the retention of strength of these two material systems after BVID.

3.1 BVID

An impact energy of 2.03 N-m (1.5 ft-lb) was used to impact the convex facesheet of all of the coupons intended for CAI testing. The resulting average dent depth was determined by dial gauge micrometer to be 0.762 mm (0.03 in). Micro-CT NDE was performed at the site of the

impact to determine the extent of the damage in the facesheet and core. Top-down images of the facesheet damage is shown in Figure 5 for coupon #46 from MTP-6003 and coupon #2 from MTP-6010. The image analysis indicated an elliptical shaped facesheet damage area of 9.42 cm^2 in MTP-6003#46 and an elliptical facesheet damage area of 10.27 cm^2 in MTP-6010#2. Side-view image analysis of the corresponding core crush damage area is shown in Figure 6 for each coupon. The analysis of buckled cells indicated that the MTP-6003 #46 coupon had an elliptical core damage area of 52.42 cm^2 and the MTP-6010 #2 coupon had a core crush area of 55.54 cm^2, both significantly greater than the facesheet dent visible to the human eye. The micro-CT NDE technique allows layer by layer analysis of the facesheet laminate. In Figure 7, an image of the +60° ply bonded to the Al honeycomb core at the FM 300 film bond-line indicates matrix cracks which are parallel to the fiber direction in this ply of the laminate in both of the coupons. The crack length in the damaged MTP-6003 #46 coupon was 19.05 mm compared to a crack length of 21.70 mm found at the same ply stack location in the MTP-6010 #2 damaged coupon. The dent depth and facesheet damage area determined using micro-CT in this study compare closely with the NDE results of BVID coupons obtained in [19] using time-of-flight, thru-transmission c-scan. Although no matrix cracking was identified using lower resolution c-scan in this previous study[18], similar matrix cracking was identified using x-radiography by Lagace in [29]. In comparing the NDE results of the two coupons fabricated using different material systems, there is less than 10% difference in any of the indicators of damage extent.

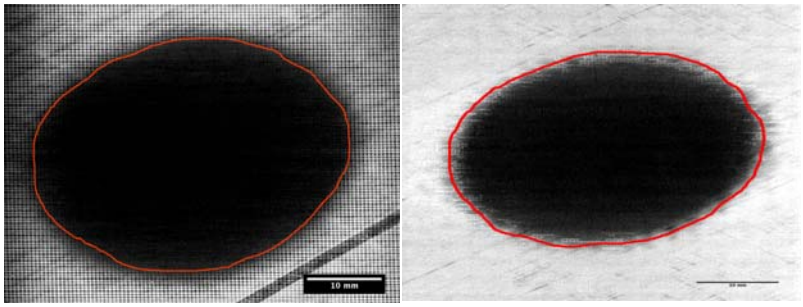

a. b.

Figure 5. Micro-CT image of facesheet surface damage after BVID in a. panel MTP-6003, coupon #46 and b. panel MTP-6010, coupon #2.

.

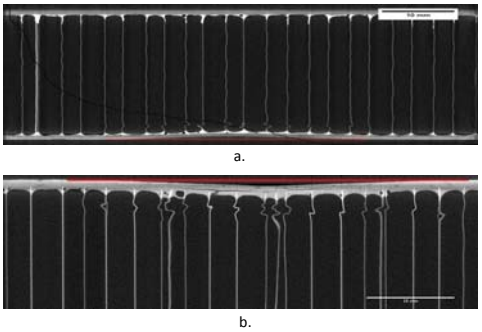

a.

b.

Figure 6. Micro-CT image of core crush damage after BVID of a. panel MTP-6003, coupon #46 and b. panel MTP-6010, coupon #2.

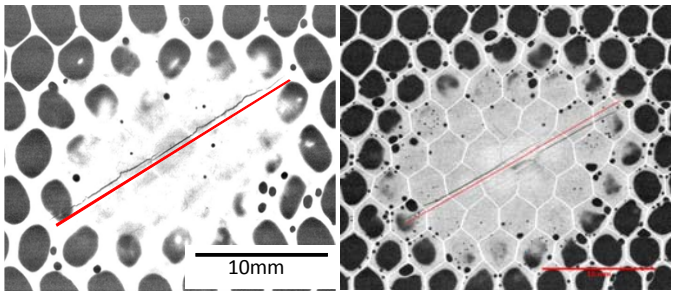

Figure 7. Micro-CT image of laminate cracking in +60° ply at the core bondline after BVID of a. panel MTP-6003, coupon #46 and b. panel MTP-6010, coupon #2.

3.2 Moisture absorption of MTP-6003 and MTP-6010 CFRP sandwich

The 35 EWC and CAI coupons from MTP-6003 and the 17 EWC and CAI coupons from MTP-6010 intended for ETW testing were divided into two groups and conditioned in a chamber. Each set of coupons was accompanied by a witness panel consisting of a 10.2 cm x 5.1 cm portion of the larger 2.0 m x 2.4 m sandwich panel. The witness panels accompanied the coupons throughout the conditioning process and were used to measure the moisture absorption of the test coupons while in the conditioning chamber. Figure 8 shows the moisture mass gained during conditioning by one of the MTP-6003 witness panels in comparison to that of the MTP-6010 witness panel. Also shown in the figure are the starting and ending points of coupon testing following the conditioning process. As shown in Figure 8, the MTP 6003 witness panel reached a mass gain of 0.912% at the beginning of coupon compression testing and was at a level of 0.916% at the end of the two weeks required to test all of the coupons from this set. Likewise, the change in mass during the six working days required to test the MTP-6010 coupons resulted in a measured mass gain of 0.001%. In comparing the moisture absorption behavior of the two different material sets, it was observed that the OOA processed MTP-6010 sandwich CFRP witness panel initially absorbed moisture at a higher rate and to a higher level than the autoclave processed MTP 6003 witness panel. The difference in mass gain between the two witness panels during testing was <0.1%.

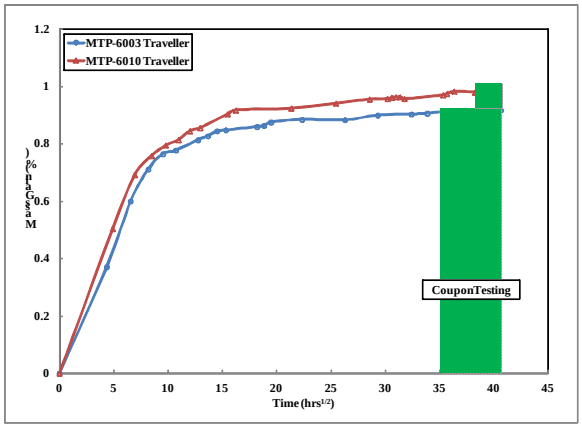

Figure 8. Moisture mass gain in witness panels from MTP-6003 and MTP-6010.

3.3 Compressive Failure Modes

The 44 undamaged coupons from both MTP-6003 and MTP-6010 that were available for EWC testing at the time of this publication exhibited the same two types of failure modes during testing. The predominant failure mode, or final damage state, was combined ply-delamination and fiber buckling/ breakage in the facesheets within the valid failure region as specified by ASTM C364 (2.54 cm above and below the top and bottom potted ends of the coupon). The failure of these coupons was denoted by a single loud pop with both facesheets typically failing at the same time across the 15.24 cm width of the coupon. Visual inspection of the failure indicated that the outer plies of each 6-ply facesheet delaminated from the inner plies, with the outer plies buckling outward and the inner plies buckling slightly inward. This was the typical failure mode for approximately 70% of the EWC coupons tested regardless of material type or test condition and is displayed in Figure 9. The other 30% of the EWC failures occurred in the same manner but within an inch of the sharp stress concentration created at the potting–coupon interface. According to the ASTM standard these are invalid failures even though the load at these invalid failures was often within the scatter of the valid failures. Due to these invalid failures, the amount of data used to calculate the average failure strength was limited; however, each test condition completed in this study contains at least two valid failures. The resulting number of coupons available after discounting the invalid failures is explained below in Section 3.4.

With the exception of two invalid failures, all 38 of the BVID CAI failed by facesheet buckling inward across the width emanating from the impact region. The majority of these failures occurred in the impacted facesheet only, as indicated in Figure 10. In two MTP-6003 coupons and one from MTP-6010, failure was observed in both facesheets. In these three cases the damaged facesheet buckled inward and the undamaged facesheet delaminated with the outer plies buckling outward and the plies closet to the core buckling inward into the Al core. The two invalid failures experienced during the CAI testing were by delamination of the potting material at the ends. Both of these failures occurred in CAI coupons from MTP-6010 tested at 105°C. Up to 80 coupons were tested in the study at the various ETW conditions before a failure of this type occurred, however, once these two invalid failures occurred in succession, it was assumed that any future coupons would have been potted without adequate surface preparation and therefore would require clamping fixtures. Testing of MTP-6010 was suspended at this point while clamping fixtures were fabricated to accommodate clamping of the potted ends of the coupons. Therefore, the data set for MTP-6010 reported below was collected using no end-clamping fixture, in identical arrangement as that of the MTP-6003 data reported.

Figure 9. Photograph of ETW EWC from MTP-6003 showing typical valid failure mode including facesheet delamination and outward buckling on both the convex and concave sides.

Figure 10. Photograph of ETW CAI from MTP-6010 showing typical facesheet buckling and core crushing valid failure mode.

3.4 Compressive Strength of undamaged and damaged CFRP Sandwich structure

The results of the EWC testing of undamaged sandwich coupons and the CAI testing of BVID sandwich coupons from both MTP-6003 and MTP-6010 panels are charted together for comparison in Figure 11. The number of valid coupon failures associated with each data column is denoted in the chart by the underlined numeral printed on each column.

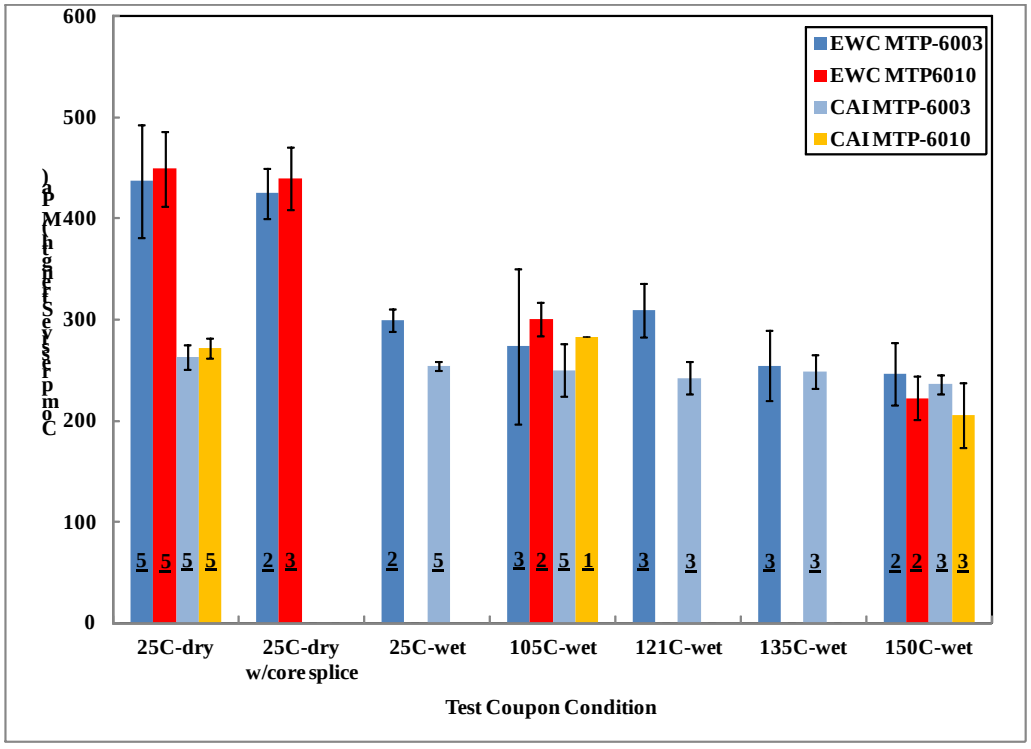

Figure 11. EWC and CAI strength of sandwich coupons tested from the autoclave processed panel MTP-6003 and the OoA processed panel MTP-6010.

The response of the sandwich coupons to compressive loads at the 25°C–dry condition for both material systems was as expected based on the literature; the BVID in the CAI coupons resulted in a retention of strength of 60% ± 1% and these results are based on five valid failures for each test set at 25°C-dry. Therefore, the compressive failure strength of the MTP-6003 and the MTP-6010 sandwich coupons in both the undamaged and BVID state are statistically equivalent at 25°C-dry. The core splice located at the center height of seven of the coupons tested at 25°C from both material sets had no significant effect on the undamaged strength for the quantity of

coupons tested in this study. Also, as expected, the moisture content at 25°C resulted in a 32% knockdown in axial compressive strength of the undamaged MTP-6003 sandwich coupons. In addition, the combination of moisture and elevated temperature resulted in a significant reduction in compressive strength of the undamaged coupons from both material systems. At the 150°C ETW testing condition, both materials have reached the level of 50% reduction in ambient undamaged compressive strength; the MTP-6003 autoclave coupons retained 56.4±7% and the MTP-6010 OoA coupons retained 50±5% of the ambient compressive strength based on the limited number of valid failures reported at the time of this publication. The most interesting results found in this study pertain to the ETW CAI coupons from panel MTP-6003. As shown in Figure 11, the failure strength at each condition from 25°C-dry BVID to 150°C BVID are statistically the same based on the standard deviation in CAI strength observed for these MTP-6003 sandwich coupons. There is no significant knockdown for the BVID coupons vs the undamaged EWC coupons at the ETW conditions. The same is true for the MTP-6010 coupons at 25°C-dry and 105°C-wet. At the 150°C-wet condition, the BVID CAI strength for the OoA material is reduced to 76% of the 25°C-dry result. These results suggest that the damage present at the BVID level is the dominant factor in the failure strength of the sandwich composite regardless of moisture absorption or thermal environment. Comparison of the average failure strength of undamaged and damaged coupons at each ETW condition from the MTP-6003 and the MTP 6010 panels indicates that the autoclave processed sandwich CFRP is equivalent in mechanical performance to the OoA processed sandwich CFRP.

4. SUMMARY AND CONCLUDING REMARKS

In a study conducted to determine alternative material options for the CFRP sandwich construction for the NASA HL-SLS payload shroud, the mechanical performance of a new OoA toughened epoxy prepreg system, Cycom® T40-800b/5320-1, was determined in conjuction with the current baseline autoclave CFRP prepreg system Cycom® IM7/977-3. The EWC and CAI coupons used in this study were sectioned from two 1/16th scale panels of the shroud 10 m barrel that were fabricated at Hitco Carbon Composites, Inc®. The CAI coupons were subjected to BVID using an impact energy of 2.03 N-m, resulting in an average dent depth of 0.762 mm for coupons of both material systems. EWC strength of the undamaged coupons and CAI of the BVID coupons was conducted at 25°C-dry and at ETW conditions ranging from 25°C to 150°C. The EWC failure strength determined for both material systems indicated a significant knockdown from the 25°C-dry strength for the moisture saturated specimens and that the ultimate failure strength continued to decrease with increasing testing temperature until the resulting failure strength reached 50% of the ambient strength at the 150°C-wet testing condition. The results of the CAI testing indicated that the BVID was a more dominant factor than the moisture or test temperature; with all of the IM7/977-3 BVID coupons exhibiting the same average CAI failure strength at 25°C-dry and at each of the ETW conditions. ETW testing of additional OoA panel specimens is ongoing. Based on the average failure strength and the associated standard deviation for the number of ETW conditioned EWC and CAI sandwich coupons tested in this study, the OoA prepreg system T40-800b/5320-1 was found to be equivalent in mechanical performance to the baseline autoclave prepreg system IM7/977-3.

5. ACKNOWLEDGEMENTS

The authors recognize the efforts of our partners in the fabrication branch at NASA LaRC, Louis Simmons and Jonny Callahan for their diligence in preparing the test coupons in this study. In addition, we acknowledge the efforts of Chris Wright and Tracy Bridges for their support to condition and test the coupons according to the ASTM standards and our direction. Especially, we acknowledge James Ratcliffe, a senior researcher at the National Institute of Aerospace, and Wade Jackson, a researcher in the LaRC Durability, Damage Tolerance, and Reliability branch, for their assistance in impacting the CAI coupons to the BVID and for their guidance throughout this effort.

6. REFERENCES

1. James, R.S., "Aluminum Lithium Alloys," ASM Handbook: Volume 2, pp.178-199, 1990.
2. Rao-Venkateswara, K.T., Yu, and R.O. Ritchie, "Fatigue Crack Propogation in Aluminum Lithium Alloy 2090: Part II Small Crack Behavior," Metallurgical Transactions A, Volume 19A, pp 563-572, 1988.
3. Bernetich, K.R., Bachman, G.N., and Louis D'Astuto, "Structural Test Comparison of Co-Cured, Skin Stiffener Composite Bonded Assemblies Using Out-Of-Autoclave & Autoclave Prepregs," Proceedings of SAMPE International Symposium, 2010.
4. Mortimer, S., Smith, M., and E. Olk," Product Development for OoA Manifacture of Aerospace Structures," Proceedings of SAMPE International Symposium, 2010.
5. Bond, G. and G.L. Hahn, "NonAutoclave Prepreg Manufacturing for Primary AerospaceStructure," Proceedings of SAMPE Technical Conference, 2009.
6. Backman, B.F., Composite Structures, Design, Safety, and innovation, Elsevier Ltd., Oxford, pp 7-15, 2005.
7. Ratcliffe, J.G. ,Jackson, W.C., and J. Schaff," Predicting the Compression Strength of Impact-Damaged Sandwich Panels," Proceedings of the American Helicopter Society 60th Annual Forum, 2004.
8. Minguet, P.J., "A model for Predicting the Behavior of Impact-Damaged Minimum Gage Sandwich Panels Under Compression," AIAA, 91-1075, 1991.
9. Shyprykevich, P., J. Tomblin, L. Ilcewicz, A.J. Vizzini, T.E. Lacy, andY. Hwang. Guidelines for Analysis, Testing, and Nondestructive Inspectionof Impact-damaged Composite Sandwich Structures. *Final Report, FederalAviation Administration Report, DOT/FAA/AR-02/121*, 2003.
10. Moody, C.and A.J. Vizzini. Damage Tolerance of Composite SandwichStructures. *Final Report, Federal Aviation Administration Report,DOT/FAA/AR-99/91*, 2000.
11. Xie, Z., A.J. Vizzini, and M. Yang. "On Residual Compressive Strength Prediction of Compressive Sandwich Panels After Low-velocity Impact Damage," *Sandwich Structures 7: Advancing with Sandwich Structures and Materials*, pages 363–372, 2005.
12. Ratcliffe, J.G., W.C. Jackson, and J. Schaff, "Predicting the Compression Strength of Impact-damaged Sandwich Panels," *Proceedings of the American Helicopter Society 60th Annual Forum, Baltimore, MD*, 2004.
13. Czabaj, M.W., Zelender, A.T., Davidson, B.D., Singh, A.K., and D.P. Eisenberg, "Compression After Impact of Sandwich Composite Structures: Experiments and

Modeling," 51st AIAA/ASME/ASCE/AHS/ASC Structures, Structural Dynamics, and Materials Conference, 2010.
14. Ransome, J.B., Glaessgen, E.H., and J.G. Ratcliffe, "An Overview of Innovative Strategies for Fracture Mechanics at NASA Langley Research Center," Proceedings of, 2010.
15. Fawcett, A.J. and G.D. Oakes," Boeing Composite Airframe Damage Tolerance and Service Experience," NIAR/FAA Workshop for Composite Damage Tolerance and Maintenance, 2006.
16. Razi, H. and S. Ward, "Principles for Achieving Damage Tolerant Composite Primary Aircraft Structures,"11th DOD/FAA/NASA conf. on Fibrous Composites in Structural Design, Ft. Worth, TX, 1996.
17. NASA- MSFC-3479, "Fracture Control Requirements for Composite and Bonded Vehicle and Payload Structures," EM20 MultiProgram/Project Common-use document, Effective Date June 29, 2006.
18. U.S. Department of Transportation-Federal Aviation Administration "Changes to original Advisory Circular on Composite Aircraft Structure," AC No: 20-107B, 08/24/2010.
19. Cvitkovich, M.K., and W.C. Jackson, "Compressive Failure Mechanisms in Composite Sandwich Structures," Journal of American Helicopter Society, Vol44 (4),pp260-268, 1999.
20. Jankowski, J.L., Wong, D.G., DiBerardino, M.F., and R.C. Cochran, "Evaluation of Upper-use Temperature of Toughened Epoxy Composites," STM STP 1249, American Society for Testing and Materials Testing and Materials, pp277-292, 1994.
21. Collings, T.A., Stone, D.E.W., " Hygrothermal Effects in CFRP Laminates: Strains Induced by Temperature and Moisture," Composites, Volume 16, Issue 4, pp. 307-316, 1985.
22. Miller,S.G., Sutter, J.K., Scheimann, D.A., Maryanski, M., and M.Schlea, "Study of Out Time on the Processing and Properties of IM7/977-3 Composites," Proceedings of SAMPE International Symposium, 2010.
23. Miller, S.G., Lort, R. D., Zimmerman, T.J., Sutter, J.K., Pelham, L.I., McCorkle, L.S., and D.A. Scheiman, "Face-sheet Quality Analysis and Thermo-Physical Property Characterization of OoA and Autoclave Panels," Proceedings of SAMPE International Symposium, 2012.
24. Ridgard, C., "Next Generation Out of Autoclave Systems," Proceedings of SAMPE International Symposium, 2010.
25. St.Clair, T.L., Johnston, N.J., and Robert M. Baucum," High Performance Composites Research at NASA-Langley," NASA-TM, 100518, 1988.
26. ASTM C364-2007, " Standard Test Method for Edgewise Compression Strength of Sandwich Construction", American Society for Testing and Materials, West Conshohocken, Pennsylvania (first issued in 1955).
27. ASTM D7136-2007, " Standard Test Method for measuring the damage resistance of a fiber reinforced polymer matrix composite to a drop-weight impact event," American Society for Testing and Materials, West Conshohocken, Pennsylvania (first issued in 2005).
28. ASTM D5229 -2010, " Standard Test Method for Moisture Absorption Properties and Equilibrium Conditioning of Polymer Matrix Composite Materials," American Society for Testing and Materials, West Conshohocken, Pennsylvania (first issued in 1992).

29. Tsang, P.H., and P.A. Lagace, Failure Mechanisms of Impact Damaged Sandwich Panels Under Uniaxial Compression," AIAA Journal, 1994, pp745-754.